ω attenuation in nuclei

P. Mühlich and U. Mosel

Institut für Theoretische Physik, Universität Giessen, D–35392 Giessen, Germany

Abstract

We study inclusive ω photoproduction in nuclei and propose a measurement of the nuclear transparency ratio as a means to learn about the in-medium properties of the ω meson. To this end we are using the semi-classical coupled-channel BUU transport approach that allows for a consistent treatment of all nuclear effects. The conditions of our calculations are chosen such as to match the setup of existing experimental facilities at ELSA or MAMI C. We show that the observables (total production cross section and transparency) indeed are sensitive to the ωN interaction in the nuclear medium.

Key words: photonuclear reactions, ω decay in nuclei, medium properties of mesons
PACS numbers: 25.20.Lj, 13.25.-k, 14.40.Cs

1 Introduction

One intriguing theme of current nuclear physics research is the change of the vector meson properties once they are embedded in a strongly interacting environment. Experimental hints towards such changes – albeit partly under much debate – have been obtained from heavy ion collisions [1,2,3] as well as from photon- [4] and proton-induced [5] reactions on finite nuclear targets. All information about the intrinsic properties of a vector meson are encoded in its spectral function. The in-medium spectral densities of the vector mesons are connected to the vector meson-nucleon and – in the case of finite temperatures – to the vector meson-pion interaction at finite ρ and/or T. Thus, they depend on information that cannot be obtained from elementary scattering processes. Whether vector mesons are – in addition – also affected by QCD condensates and their in-medium changes [6,7,8] is still a matter of debate.

In the present paper we concentrate on the spectral density in the vector-isoscalar channel. Theoretical results for the ω in-medium spectral function have been obtained on the basis of rather different methods [9,10,11,12,13]. The outcome of these models covers a large area in the mass/width plane, ranging for the mass from the free ω pole at $m_0 = 782$ MeV down to roughly 640 MeV for an ω meson at rest in nuclear matter at saturation density ρ_0. For the width, that amounts to $\Gamma_0 = 8.4$ MeV in vacuum, in-medium values of up to about 70 MeV at ρ_0 have been obtained. The origin of the ω medium modifications at finite density and zero temperature have for instance been attributed to the collective excitation of resonance-hole loops [12,13] that lead to additional structures in the spectral function. Another source of medium modifications can be the renormalization of the pion cloud, considered in [10,11], that results in a rather drastic shift of spectral strength to the low mass region.

One photoproduction experiment with the aim to learn about the ω in-medium spectrum has been done only recently at ELSA [4]. $\pi^0\gamma$ pairs from ω mesons photoproduced in finite nuclear systems have been detected in order to reconstruct the invariant mass spectrum of the decayed ω mesons. The $\pi^0\gamma$ decay mode is particularly sensitive to the vector-isoscalar channel as the anomalous coupling $\omega - \pi^0\gamma$ is rather large [14]. In a preceding paper [15] we have shown that despite the strong final state interactions of the outgoing pion it is possible to obtain information on the ω in-medium spectrum from such a measurement. Whereas the authors of [4] report a downward shift of the ω in-medium peak, the assignment of an in-medium width was not possible due to the only moderate detector resolution. Even cleaner signals for the in-medium change of the vector meson properties are expected from an observation of the dilepton yield as this final state is essentially free of any final state interactions. The analysis of such an experiment done at JLAB is presently under way [16].

An alternative method to study the ω self energy in nuclei is an attenuation measurement of the ω flux in ω photoproduction off nuclei. Already in early experiments on the ρ meson properties in nuclei [17] this method has been used to yield the first extraction of the ρN cross section from photoproduction experiments on nuclei. More recently, the authors of [18] haven taken this up for the case of ϕ photoproduction. In [19] we have shown that the A-dependence of the total ϕ meson yield is indeed sensitive to the ϕ width in the nuclear medium. Data taken at SPring8/Osaka [20] show the need for an explicitly higher ϕ absorption cross section as compared to usual quark model estimates in order to obtain agreement between theory and experiment. In the present paper we take over the same idea in order to show the possibility to obtain information on the ωN interaction in nuclei via a measurement of the $\pi^0\gamma$ yield from photon-nucleus reactions. Such experiments are presently being evaluated.

This article is structured in the following way: In the following section we introduce the semi-classical framework that we use to model inclusive particle production in photon nucleus reactions. In section 3 we discuss our results that are structured according to different scenarios of medium modifications. Finally we turn to the discussion of ω photoproduction in nuclei within the semi-analytic Glauber model and show its power in analyzing our previously obtained transport results. We close with a summary in section 5.

2 Model

2.1 Transport Model

In order to simulate the production and propagation of ω mesons in finite nuclear targets in an as realistic way as possible we employ the semi-classical Giessen BUU transport approach. This approach describes incoherent photon-nucleus reactions and has successfully been applied previously to the study of medium modifications of the ρ, ω and ϕ mesons by means of e^+e^- [21], $\pi^0\gamma$ [15] and K^+K^- [22,19] photoproduction in nuclei. The model aims at a complete description of all nuclear effects, i. e. Fermi motion, Pauli blocking, nuclear shadowing, strong and electromagnetic potentials and elastic and inelastic scattering processes including sidefeeding and regeneration of all propagated particles. Moreover, not only the elastic, but also inelastic production channels, i. e. $\gamma N \rightarrow VX$ ($X = \pi N, \pi\Delta, ...$), are included by means of nucleon resonance decay channels or the LUND model FRITIOF [23]. A description of the Giessen BUU model can be found in Refs. [21,22,24,25,26] and references therein. In [19] we have demonstrated the necessity to carefully account for rescattering processes and hadronic potentials in order to reliably extract the ϕN interaction strength from ϕ photoproduction experiments.

The ω photoproduction cross section at finite density we calculate by allowing the ω meson to take arbitrary masses and convoluting the obtained expression with the ω spectral function at given density. The matrix element we calculate within a tree-level model, including the contribution from the t-channel π-exchange as well as the s- and u-channel contributions including the nucleon and the $P_{11}(1710)$ as intermediate states following the findings of [27]. In vacuum, this model describes the experimentally determined angular distributions very well. The more complicated structures in the total cross section [28] are, however, hard to obtain within such a simple approach. For the total production rate we therefore use the measured cross section as obtained by the SAPHIR collaboration [28]. The implementation of this experimental information into our transport simulation is explained in [15]. There also the inclusion of inclusive photoproduction channels is discussed. Due to the lack of
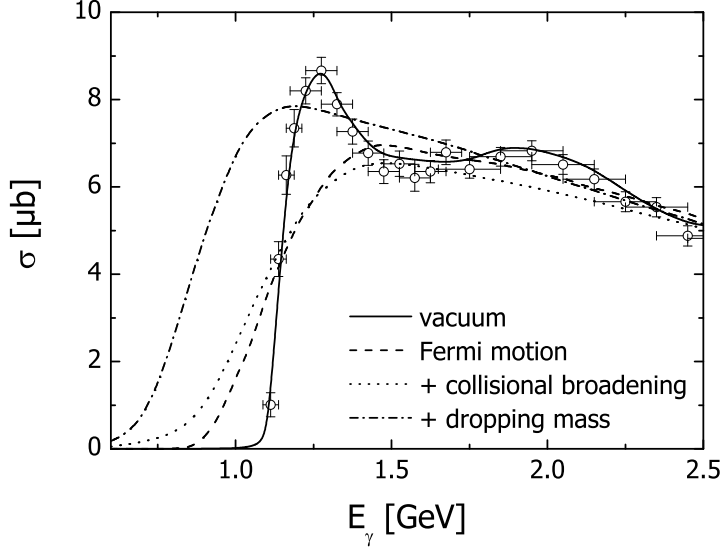
Fig. 1. Total exclusive ω photoproduction cross section on the nucleon. For the dashed curve the effect of Fermi motion at normal nuclear matter density ρ_0 has been taken into account. The dotted and dash-dotted curves in addition include medium modifications according to Eqs. (3), (5). The data points are taken from [28].

experimental information we assume the cross section from neutrons to be the same as the cross sections from protons. In Fig. 1 the exclusive cross sections from the proton target in vacuum as well as at non-zero density, assuming different scenarios of medium modifications of the ω that will be subject to the following discussions, are shown.

2.2 The ωN interaction

In the very same spirit as in a preceding paper for the case of ϕ photoproduction [19] we use parametrization for the ωN total cross sections. For ωN elastic scattering we have

$$\sigma_{\rm el} = [5.4 + 10 \exp\left(-0.6 \left|\mathbf{q}\right|\right)] \ {\rm mb} \tag{1}$$

where $\mathbf{q}$ is the laboratory momentum of the ω meson in GeV. This expression has been obtained in [29] by an interpolation of the low energy cross section, calculated from a microscopic model, and the high energy limit obtained within an additive quark model. Also for the inelastic cross section we use the parametrization from [29]

$$\sigma_{\rm in} = \left[20 + \frac{4}{\left|\mathbf{q}\right|}\right] \ {\rm mb}, \tag{2}$$

that again interpolates the low energy cross section, given by the sum of the individual contributions $\omega N \to \pi N, 2\pi N, \sigma N, \rho N$ and $\rho\pi N$, and the high energy limit, estimated within the strict vector meson dominance model (SVMD). For high energies ($\sqrt{s} > 2.2$ GeV) inelastic scattering events are simulated within the FRITIOF model [23]. Both the cross sections (1) and (2) are obviously only estimates. However, more recent coupled-channel analysis of pion- and photon-induced ω production cross sections on the nucleon [30] yield results that are comparable in magnitude with those of [29] although they fall of with momentum more quickly than (2). Ultimately, attenuation experiments can help to determine at least the inelastic cross section.

The collisional width of the ω we obtain via the low density theorem within a local density approximation

$$\Gamma_{\text{coll}}(q_0 = \sqrt{m_V^2 + \mathbf{q}^2}, \mathbf{q}; \rho(\vec{r})) = \frac{4}{m_V} \int \frac{d^3p}{(2\pi)^3} \Theta(|\mathbf{p}| - p_F(\vec{r}))$$
$$\times \frac{k\sqrt{s}}{E_N(\mathbf{p})} \sigma_{VN}(s) \qquad (3)$$

with k being the center-of-mass momentum of nucleon and ω, E_N the nucleon on-shell energy in the laboratory frame and $p_F(\vec{r})$ the local Fermi momentum. The cross section σ_{VN} is the total ωN cross section containing all quasi elastic and absorption channels. For ω mesons at rest we find a collisional width of 37 MeV at normal nuclear matter density, a value that lies within the range of most of the more elaborate approaches [11,12,13]. We note, however, that we assume in our calculations a Breit-Wigner shape for the spectral function of the ω and thus do not allow for a multi-humped structure as obtained in [12,13].

3   Results

3.1   Observables

As a measure for the ω width in nuclei we use the so-called nuclear transparency ratio:

$$T_A = \frac{\sigma_{\gamma A \to VX}}{A \sigma_{\gamma N \to VX}} \ , \qquad (4)$$

i. e. the ratio of the inclusive nuclear ω photoproduction cross section divided by A times the same quantity on a free nucleon. It can be interpreted as the
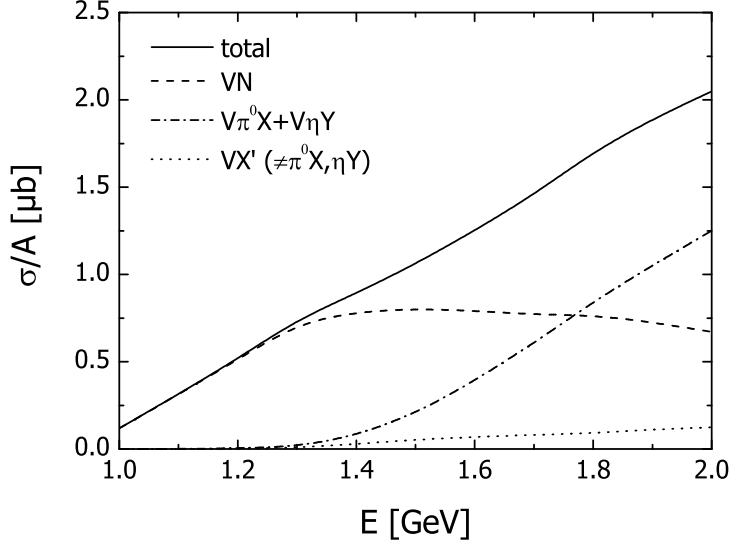
Fig. 2. Total inclusive $\omega \to \pi^0 \gamma$ photoproduction cross section from ^{40}Ca *without* final state interactions and Pauli blocking. The dash-dotted line gives the cross section for the production of inclusive final states including a π^0 or an η meson. The dashed line, labeled VN, gives the $\gamma A \to \omega A \to \pi^0 \gamma A$ cross section.

momentum- and position-space averaged probability of an ω meson to get out of the nucleus. The loss of flux is obviously related to the absorptive part of the ω nucleus potential and thus to the ω width in the nuclear medium.

Moreover, the total nuclear production cross section and the transparency ratio can also be sensitive to the real part of the ω nucleus potential. An attractive mass shift, e. g. of the Brown-Rho-type [6]

$$m_V^* \equiv m_V^*(\mathbf{r}) = m_V^o \left[1 - \alpha \frac{\rho(\mathbf{r})}{\rho_0} \right] \ , \tag{5}$$

where $m_V^o = 782$ MeV is the physical ω mass in vacuum, causes an in-medium lowering of the ωN threshold due to the smaller ω mass at finite density. This results in a divergent transparency ratio at the vacuum threshold and an explicit enhancement in the near threshold region. We note, however, that such a threshold enhancement is not a unique signal for a lowering of the in-medium ω mass but can also – albeit weaker – be generated by Fermi motion and coherent nuclear ω production. We will discuss this issue in more detail among the results of our calculations.

3.2 Imaginary part of the ω nucleus potential

In order to first explore the imaginary part of the ω nucleus potential, we perform calculations at the fixed photon beam energy of $E_\gamma = 1.5$ GeV. On
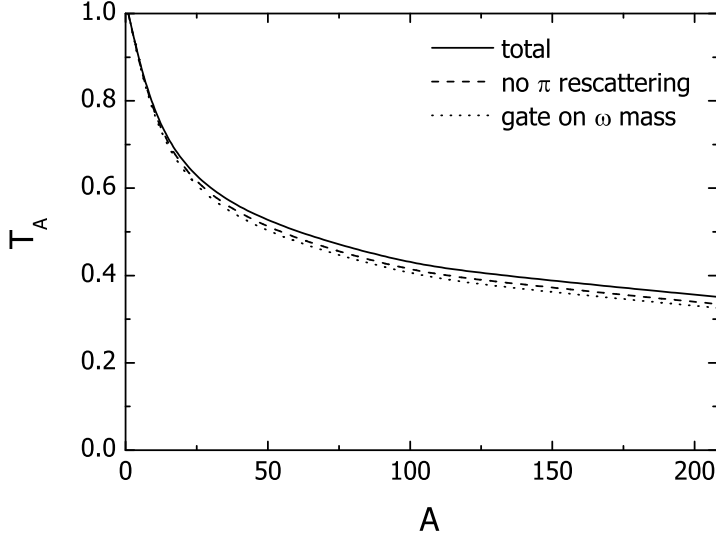
Fig. 3. Nuclear transparency ratio from BUU calculations as function of the target mass number. The photon energy is $E_\gamma = 1.5$ GeV. The solid curve is calculated without any restrictions on energy and momentum of the $\pi^0\gamma$ pair. For the dashed line pions that interacted via a quasi elastic collision are removed from the flux. For the dotted line in addition the $\pi^0\gamma$ invariant mass has been restricted to 0.75 GeV $\leq M \leq 0.81$ GeV.

one hand, this energy is well above the free production threshold (≈ 1.1 GeV) so that here one is essentially free of any threshold effects, i. e. medium modifications of the elementary cross section for instance due to the in-medium broadening of excited nucleon resonances. Also the sensitivity to a density-dependent shift of the ω pole mass becomes small for this beam energy as we will show in the following section. On the other hand, the chosen energy is low enough so that any inclusive production channels $\gamma N \rightarrow VX$ with $X \neq N$ (dotted line in Fig. 2) are of minor importance. Moreover, events from the dominant inclusive channel $\gamma N \rightarrow V\pi^0 X$ can easily be suppressed experimentally. Thus, ambiguities due to the elementary production process are minimized for the chosen beam energy of 1.5 GeV.

The BUU calculations have been performed for the targets ^{12}C, ^{40}Ca, ^{93}Nb, ^{120}Sn and ^{208}Pb with an eye on the TAPS experiment where the ω is detected via the $\pi^0\gamma$ decay channel. In Fig. 3 we show our results obtained within the standard scenario, i. e. using the cross sections as given by Eqs. (1), (2) and including collisional broadening of the ω according to Eq. (3) as a medium modification only. In the experimental analysis one tries to get rid of pions that rescattered in the medium since these $\pi^0\gamma$ pairs essentially lose all information about their source. This can be done easily as these $\pi^0\gamma$ pairs appear at much lower values of the invariant mass and also the π kinetic energy is smaller as compared to pions from the ω decay that leave the target nucleus untouched [31,15]. Removing the pions that interacted via quasi elastic collisions from the total flux, we obtain the dashed line in Fig. 3, i. e. only a small reduction
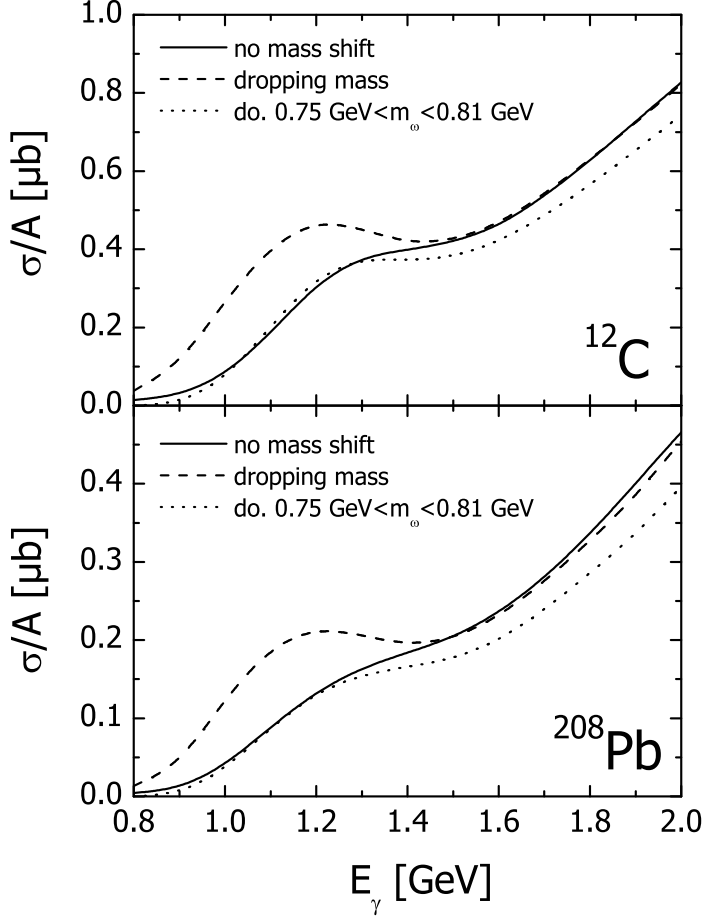
Fig. 4. Total ω photoproduction cross section from ^{12}C and ^{208}Pb as function of the photon beam energy. Results with and without a density dependent shift of the in-medium ω are shown. The dotted curves are obtained by imposing the condition that 0.75 GeV $\leq M \leq 0.81$ GeV.

of the transparency ratio is observed. This becomes immediately clear if one realizes that most of the ω mesons decay outside the nucleus and therefore the probability for the pion to scatter from the target nucleons is small. If, in addition, restrictions on the $\pi^0\gamma$ invariant mass are imposed in order to gate on the ω decay component in the $\pi^0\gamma$ spectrum, only a slight reduction can be observed. This is shown by the dashed curve in Fig. 3, where the condition 0.75 GeV $\leq M \leq 0.81$ GeV has been applied. Again the reason for this marginal effect is the only tiny contribution of ω decays in the medium where the ω spectral distribution becomes broad.

3.3 Real part of the ω nucleus potential

In order to obtain also information on the real part of the ω nucleus potential, one has to examine the energy dependence of the total cross section in the
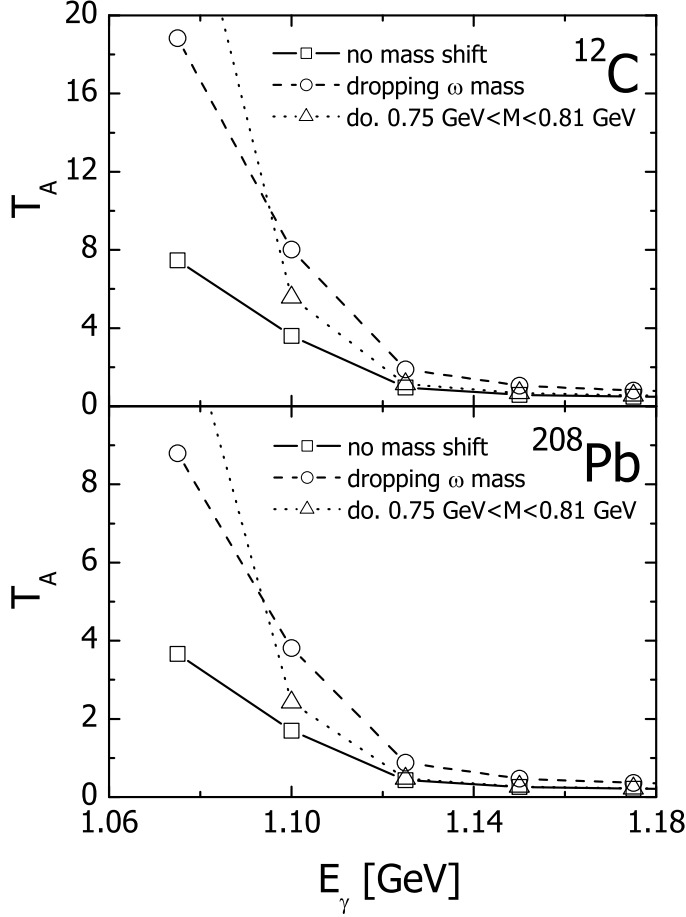
Fig. 5. Nuclear transparency ratio as function of the photon energy in the threshold region. Results with and without a density-dependent shift of the in-medium ω mass are shown. The dotted curves are obtained by imposing the condition that $0.75 \text{ GeV} \leq M \leq 0.81 \text{ GeV}$.

threshold region. This is shown in Figs. 4 and 5, where results with and without a density dependent shift of the ω pole mass for the targets ^{12}C and ^{208}Pb are shown. The real part of the ω in-medium self energy we parametrize by the attractive mass shift as given in Eq. (5) with the canonical strength parameter $\alpha = 0.16$ [7,10], that is also consistent with the measurement of the in-medium ω mass reported in [4]. At low photon energy the cross section including the dropping ω mass shows a pronounced excess over the standard calculation due to the lowering of the ωN threshold in the medium. However, the transparency ratio shows an enhancement towards the ωN threshold[1] already without any real ω potential due to the in-medium broadening of the ω spectral function and the energy smearing caused by Fermi motion. The threshold enhancement is magnified when the attractive mass shift according to Eq. (5) is turned on.

---

[1] Also the diminishing recoil due to coherent ω production would lead to a shift of the threshold with the mass number A. This shift, however, does not show up in the quasielastic events considered here.

The production of ω mesons at energies below the free production threshold is dominated by the low-energy tail of the ω in-medium spectral function. Such ω mesons far off-shell the free ω mass are difficult to identify experimentally, but they do contribute to the total ω yield and thus influence the transparency ratio. Therefore, we again show results with the condition 0.75 GeV $\leq M \leq$ 0.81 GeV. Imposing this restriction on the $\pi^0\gamma$ mass, the component of low-mass ω mesons in the final particle yield is discarded. That the dotted curve in Fig. 5 shows a strong rise at small energies is due to the fact that here the mass-cut influences the elementary cross section even more than the nuclear one. Cutting out the low mass tails of the spectral function of the free ω leads to the drastic rise, which is thus not an in-medium effect.

However strong the threshold enhancement shows up, any extraction of the real part of the in-medium self energy has to relie on the solid line in Fig. 5 as a baseline. This, however, is extremely sensitive to the theoretical assumptions for the ω photoproduction cross section. Thus, a complete understanding of the elementary production process is required. Theoretical efforts towards such a complete description of ω photoproduction from elementary targets are, however, underway [30]. At present, a unique mapping of the observed effects to particular medium modifications turns out to be difficult as the relevant contributions to the ω photoproduction process have not yet been resolved.

3.4   Medium modifications of the ω decay width

As for the ω also the spectral function of the ρ meson is expected to change in the nuclear medium [10,32,33,34]. Such a modification of the in-medium ρ spectrum has also an impact on the ω self energy as the most important decay channel of the ω in vacuum is $\omega \to 3\pi$ that is dominated by the Gell-Mann-Sharp-Wagner (GSW) process, a process where the ω first converts into an intermediate $\rho\pi$ state followed by the decay of the virtual ρ into two pions. The $\omega \to 3\pi$ decay width then is given by

$$\Gamma_{\omega \to 3\pi}(s, \rho) = \frac{3g^2}{4\pi m_\pi^2} \int\limits_{4m_\pi^2}^{(\sqrt{s}-m_\pi^2)^2} dm_\rho^2 \; q^3 \mathcal{A}_\rho(m_\rho, \rho) \frac{\Gamma(\rho \to \pi\pi)}{\Gamma_{\text{tot}}(m_\rho, \rho)}, \tag{6}$$

where $\mathcal{A}_\rho$ is the (in-medium) spectral function of the ρ meson and Γ_{tot} is its total (in-medium) width. The $\omega - \rho\pi$ coupling constant g is determined by the postulate that at the on-shell point the experimental width of 7.5 MeV [35] is obtained. The phase-space factor q is given by the center-of-mass momentum of the virtual ρ meson and pion:
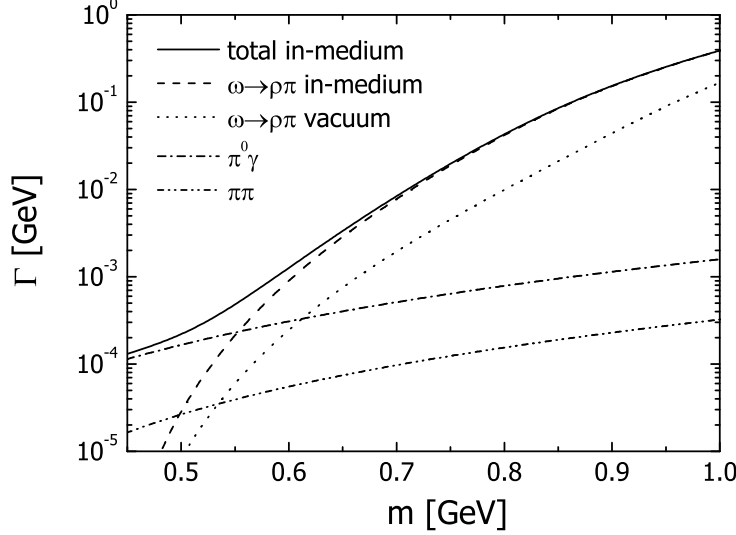
10

Fig. 6. Partial and total decay widths of the ω meson in vacuum and at normal nuclear matter density. The ω collisional width is not included. At the on-shell point the $\rho\pi$ decay width amounts to 7.5 MeV in vacuum, whereas at ρ_0 it increases to 31.8 MeV.

$$q \equiv p_f(s, m_\rho, m_\pi) = \sqrt{\frac{1}{4s}\left((s - m_\rho^2 - m_\pi^2)^2 - 4m_\rho^2 m_\pi^2\right)}, \tag{7}$$

where s is the mass of decaying ω meson squared and m_ρ is the mass of the virtual ρ meson. For the vacuum spectral density of the ρ meson we take its coupling to a 2π state into account. The ρ decay width to this channel is given by [14]

$$\Gamma(\rho \to \pi\pi) = \frac{f_\rho^2}{48\pi} m_\rho \left[1 - 4\frac{m_\pi^2}{m_\rho^2}\right]^{\frac{3}{2}}, \tag{8}$$

where again the coupling is obtained from the experimental ρ width of 149.2 MeV. Due to the dependence of the phase-space factor q^3 on m_ρ only the low-energy tail of the ρ spectral function contributes to the integral in Eq. (6). Therefore the $\omega \to 3\pi$ width increases dramatically for higher ω masses as more and more of the ρ strength is picked up by the integral.

Going to the nuclear medium, the ρ spectral distribution is broadened due to elastic and inelastic ρN collisions that lead to a shorter lifetime of the interacting ρ state. We include this broadening by adding the phenomenological collisional width of roughly 100 MeV at normal nuclear matter density [21] to the total ρ width in the medium:

$$\Gamma_{\text{tot}}(m_\rho, \rho) = \Gamma(\rho \to \pi\pi) + 0.1 \text{ GeV} \cdot \frac{\rho}{\rho_0}. \tag{9}$$
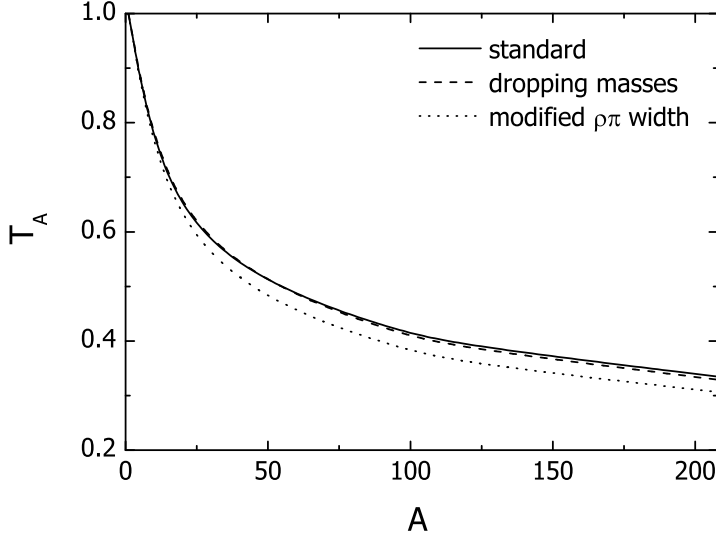
11

Fig. 7. Nuclear transparency ratio at $E_\gamma = 1.5$ GeV. The dashed and dotted lines include dropping vector meson masses. For the dotted line in addition the modification of the $\omega \to \rho\pi$ decay width has also been taken into account.

On top of that we also consider a dropping ρ mass analogous to the dropping ω mass in matter given by Eq. (5). We note that not only a shift of the ρ pole mass but also a very general reshuffling of spectral strength to the low energy part of the ρ spectral function would result in a similar effect on the ω decay width. Such a shift of strength could be caused by the excitation of subthreshold nucleon resonances as for instance obtained in the sophisticated approach of Ref. [34]. Our result at normal nuclear matter density excluding the ω collisional width is shown in Fig. 6. Due to the fact that more of the spectral strength of the ρ meson lies inside the bounds of the integration in Eq. (6), the $\rho\pi$ width of the ω increases from 7.5 MeV in vacuum to 31.8 MeV at normal nuclear matter density.

In Fig. 7 we show the nuclear transparency with and without including the modified $\omega \to \rho\pi$ decay width on top of the ω collisional width. The dropping ρ and ω masses alone have no effect on the transparency ratio as the photon energy is well above threshold where the change in the phase space factors becomes small. Including the modified $\rho\pi$ decay width, more ω mesons decay to that channel due to the opening of the $\rho\pi$ phase space at non-zero nuclear density. Hence more ω mesons are taken out of the total flux inside the nucleus. This leads to a further but small reduction of the transparency ratio.

3.5   Sensitivity to the ωN absorption cross section

In view of the uncertainties connected with the ωN cross section we show in Fig. 8 our results for the transparency ratio using different assumptions for
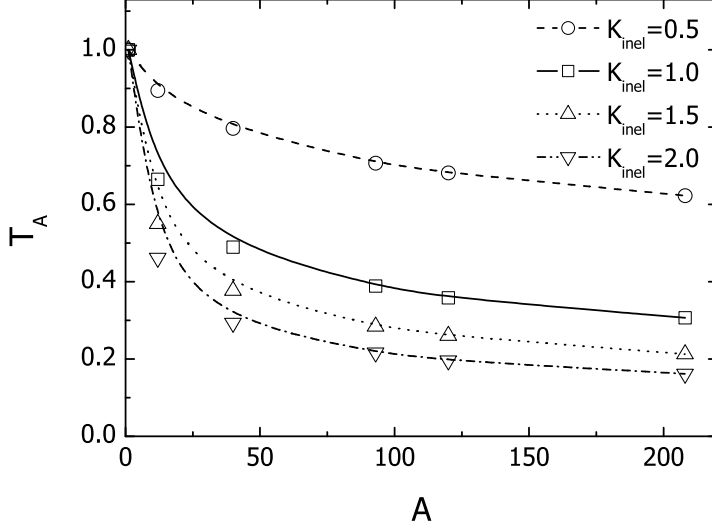
Fig. 8. Nuclear transparency ratio obtained from BUU transport simulations as function of the target mass number. Calculations have been done for different inelastic K-factors. The photon energy is $E_\gamma = 1.5$ GeV. No acceptance corrections have been applied.

the ω collisional width. To this end we multiply the collisional part of the ω self energy with a constant normalization K-factor. According to the low density theorem (3), a modification of the collisional width goes along with an analogous change of the total ωN cross section, i. e.

$$\tilde{\Gamma}_{\text{coll}} = K_{\text{inel}} \cdot \Gamma_{\text{coll}} \leftrightarrow \tilde{\sigma}_{VN} = K_{\text{inel}} \cdot \sigma_{VN} \ . \tag{10}$$

In the present calculations, we put this modification entirely into the absorptive part of the ω self energy, i. e.

$$\tilde{\sigma}_{VN}^{\text{inel}} = K_{\text{inel}} \cdot \sigma_{VN}^{\text{tot}} - \sigma_{VN}^{\text{inel}} \tag{11}$$
$$\tilde{\sigma}_{VN}^{\text{el}} = \sigma_{VN}^{\text{el}} \ , \tag{12}$$

where σ_{tot} is the sum of the elastic and inelastic channels. After all, the transparency ratio without any restrictions on angles and momentum of the produced particles will be sensitive primarily to the absorptive part of the ωN interaction as quasi elastic scattering processes do not lead to a loss of flux.

Besides the results obtained with the canonical value for the ω in medium width ($K_{\text{inel}} = 1.0$, $\Gamma_{\text{coll}} = 37$ MeV), curves with $K_{\text{inel}} = 0.5$, $K_{\text{inel}} = 1.5$ and $K_{\text{inel}} = 2.0$ are shown. We also include the dropping ρ and ω masses as well as the modified $\rho\pi$ decay width as discussed previously. The results from our transport calculations show an obvious lowering of the nuclear transparency ratio as the ω width goes up and, hence, the mean free path of the ω shrinks to smaller values. The transparency ratio decreases in a non-linear way with the
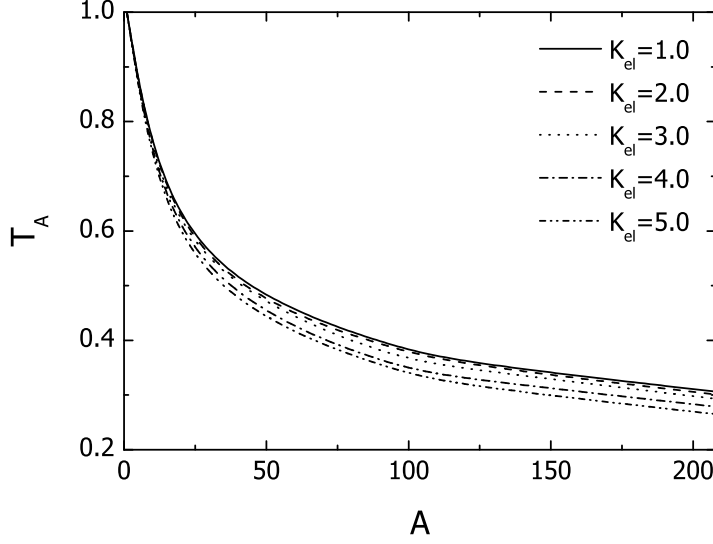
13

Fig. 9. Nuclear transparency ratio at $E_\gamma = 1.5$ GeV. Calculations for different elastic K-factors from $K_{el} = 1.0$ to $K_{el} = 5.0$ are shown.

increasing ω width. Whereas the absolute size of the transparency ratio yields important information about the ω collisional width, its A-(N-, Z-) scaling in principle is also sensitive to the isospin dependence of the production and absorption cross sections.

3.6 Elastic scattering

Finally, we explore the influence of different assumptions for the ωN elastic scattering cross section on the nuclear transparency. Again we use a constant normalization factor K_{el} that we now multiply to the elastic scattering cross section

$$\tilde{\sigma}^{el}_{VN} = K_{el} \cdot \sigma^{el}_{VN} \tag{13}$$
$$\tilde{\sigma}^{tot}_{VN} = \tilde{\sigma}^{el}_{VN} + \sigma^{inel}_{VN}. \tag{14}$$

As said earlier, elastic scattering processes do not lead to a loss of flux and, thus, do not directly influence the total nuclear cross section and the transparency. On the other hand, such scattering processes change the ω momentum distribution and, therefore, help to keep the ω mesons inside the medium for a longer time. The stopping of the ω mesons in nuclear matter due to elastic ωN scattering is particularly large as the mass of the ω is comparable to the nucleon mass, what leads to a relatively high energy loss of the ω in these collisions.

The transparency ratio with normalization factors $K_{el} = 1, 2, 3, 4$ and 5 is shown in Fig. 9. The impact of the different elastic K-factors indeed is small.
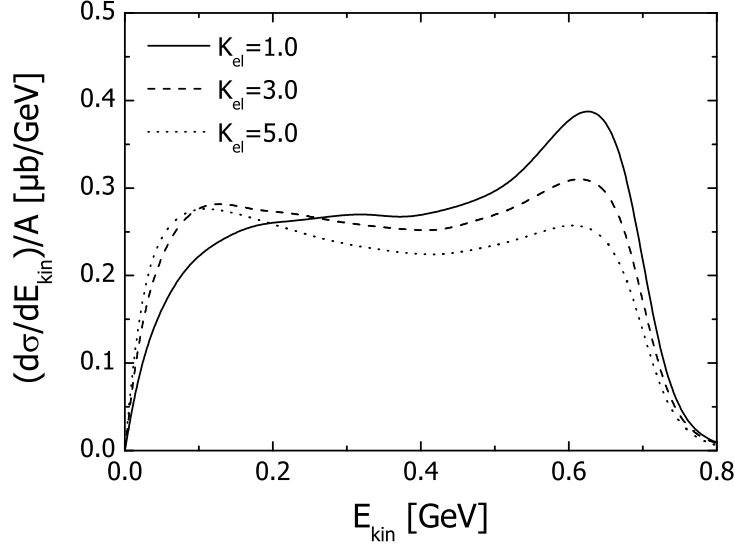
Fig. 10. Kinetic energy spectra of $\pi^0\gamma$ pairs from ^{208}Pb at $E_\gamma = 1.5$ GeV.

In Fig. 10 we also show the kinetic energy spectra resulting from these calculations, here for the case of the ^{208}Pb target. The peak at high kinetic energies is due to the forward peaked angular distribution for the $N(\gamma, \omega)N$ process. Turning on elastic ωN scattering, ω mesons from the high energy part of the spectrum are shuffled to the low energy tail. On one hand, these ω mesons stay in the medium for a longer time where they have the chance to get absorbed in inelastic ωN collisions. On the other hand, the ωN absorption cross sections are particularly large at low energies due to the open phase space at the ωN threshold for processes like $\omega N \to \pi N$, $\omega N \to \pi\pi N$ etc. Hence, we observe a slight reduction of the nuclear transparency with the increasing elastic ωN cross section. Note, that the effect on the transparency ratio becomes significant only for K-factors $K_{el} = 4, 5$ what means a rather drastic change of the elastic scattering cross section as compared to our standard estimate Eq. (1).

3.7 Final remarks

At first glance it appears to be quite astonishing that the enhanced collisional width has a much larger impact on the transparency than a modification of the $\omega \to \rho\pi$ decay channel. The reason for this effect lies in the momentum dependence of both contributions to the in-medium self energy. In our model the ω collisional width is – except for the threshold region where the nucleon momentum distribution plays an important role – proportional to the ω momentum with respect to the nuclear medium. Thus the collisional width of roughly 37 MeV at normal nuclear matter density for ω mesons at rest blows up to almost 150 MeV for a typical laboratory momentum of 1 GeV. In contrast, the modification of the $\rho\pi$ decay width generated by the purely

15

density-dependent ρ meson potential is independent of the ω momentum. In the considered photon energy regime, the ω momentum distribution is peaked around $p = 1$ GeV. Hence, a doubling of the inelastic collisional self energy ($K_{inel} = 1 \rightarrow K_{inel} = 2$) has an effect on the ω attenuation that is roughly one order of magnitude larger than the impact of the decreasing ρ meson mass.

In fact, the nuclear transparency is sensitive not only to the ωN interaction in nuclei but also to medium modifications of the production processes and decay widths of the ω meson. In particular, also the ω production rates from neutrons have to be known in order to obtain precise information on the ω nucleus potential. In view of that, it might be desirable to normalize the nuclear transparency ratio not to the proton cross section but to the ω yield obtained from Deuterium or Carbon targets. Further uncertainties concerning the determination of the real as well as the imaginary part of the ω nucleus potential arise from the possibility that also the $\pi^0\gamma$ decay width as well as other decay channels might become modified in a surrounding with non-zero nuclear density. In particular the change of the ρ spectral function in nuclei and its back coupling on the ω in-medium self energy are still open issues. Experimentally, it is essential to understand the background so that the actual production cross section (that is not necessarily required for a verification of a shape change of the ω in-medium spectral function) and, correspondingly, the transparency are quantitatively reliable.

4   Glauber approximation

In this section we will finally discuss ω photoproduction in the semi-analytic Glauber picture as a much simpler means to extract the inelastic ωN cross section from the total photoproduction cross section. After our detailed study of various nuclear effects within the coupled channel transport approach, we have found that the nuclear transparency ratio at photon energies well above threshold is first of all sensitive to the ωN absorption cross section whereas other medium effects such as dropping vector meson masses and the modified decay width give rise to only small corrections. We note, however, that this statement holds only as long as total inclusive observables without any cuts on angle and momentum of the observed vector mesons are considered. A limited experimental acceptance possibly introduces dependences on elastic scattering processes and details of the dynamics that cannot be included in the semi-analytic Glauber framework.

4.1 Analytic expressions

In the Glauber-eikonal approximation, neglecting Fermi motion, Pauli blocking, coupled-channel effects, nuclear shadowing and quasi elastic scattering processes, the incoherent single meson photoproduction cross section has the following form [19]:

$$\sigma_{\gamma A} = \int d^3 r \rho(\mathbf{r}) \sigma_{\gamma N} \exp\left[-\sigma_{VN}^{\text{inel}} \int\limits_z^\infty dz' \rho(\mathbf{b}, z')\right] . \qquad (15)$$

where $\rho(\mathbf{r})$ is the nuclear density distribution, $\sigma_{\gamma N}$ the total vector meson photoproduction cross section on a single nucleon and $\sigma_{VN}^{\text{inel}}$ ($\equiv \sigma_{VN}$ in the following) the vector meson nucleon absorption cross section. In Eq. (15) we have neglected any π final state interactions which, anyway, give only marginal corrections to the nuclear cross section as most of the ω mesons decay outside the nucleus.

In order to carry out the integrals explicitly we approximate the nuclear density distribution by a sphere that is filled up homogeneously with A nucleons

$$\rho(\mathbf{r}) = \rho_0 \Theta(|\mathbf{r}| - R) = \frac{3A}{4\pi R^3} \Theta(|\mathbf{r}| - R), \qquad (16)$$

where R is the nuclear radius that we parametrize according to $R = r_0 \cdot A^{1/3}$. For the radius parameter r_0 we use the numerical value $r_0 = 1.143$ fm in order to be consistent with $\rho_0 = 0.16$ fm^{-3}. Going to cylindrical coordinates and assuming that the elementary cross section does not depend on the density, we are then able to rewrite Eq. (15) in the following way:

$$\sigma_{\gamma A} = \int d^2 b \, dz \, \frac{\sigma_{\gamma N}}{\sigma_{VN}} \frac{\partial}{\partial z} \exp\left[-\sigma_{VN} \int\limits_z^\infty dz' \rho(\mathbf{b}, z')\right] \qquad (17)$$

where now $\mathbf{b}$ is the 2-dimensional coordinate in the plane perpendicular to the incoming photon direction. At this stage we introduce one further abbreviation, namely

$$\lambda_0 = \frac{1}{\sigma_{VN} \rho_0} \qquad (18)$$

which is the mean free path of the vector meson at normal nuclear matter density with respect to inelastic vector meson nucleon collisions. Evaluating Eq. (17) further we obtain
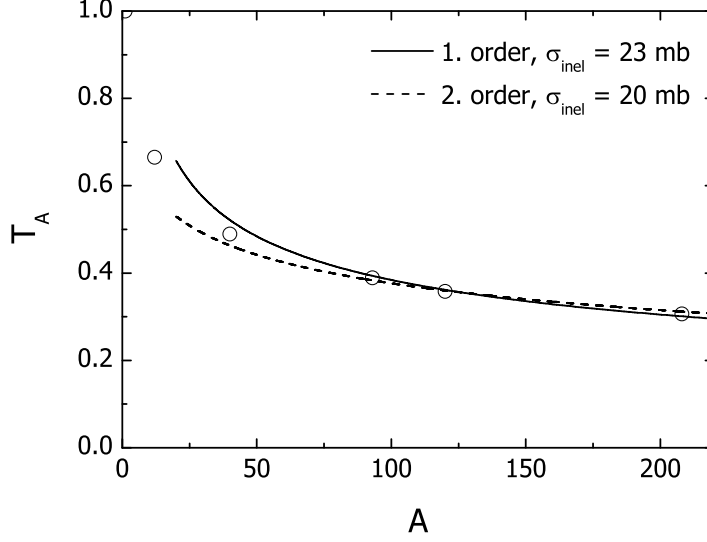
Fig. 11. Nuclear transparency ratio according to Eq. (21) fitted to BUU calculations (open circles) from Fig. 8 with $K_{\mathrm{inel}} = K_{\mathrm{el}} = 1$. For details see text.

$$\sigma_{\gamma A} = 2\pi \frac{\sigma_{\gamma N}}{\sigma_{VN}} \int\limits_0^R b \, db \left\{ 1 - \exp\left[-\frac{1}{\lambda_0} \int\limits_{-\infty}^{+\infty} dz' \Theta(\sqrt{b^2 + z'^2} - R) \right] \right\} \tag{19}$$

$$= \pi R^2 \frac{\sigma_{\gamma N}}{\sigma_{VN}} \left\{ 1 - \frac{2}{R^2} \int\limits_0^R b \, db \exp\left[-2\frac{\sqrt{R^2 - b^2}}{\lambda_0} \right] \right\}. \tag{20}$$

Carrying out the remaining integral, we finally obtain the following expression for the nuclear transparency ratio:

$$T_A = \frac{\pi R^2}{A \sigma_{VN}}$$
$$\times \left\{ 1 + \left(\frac{\lambda_0}{R} \right) \exp\left[-2\frac{R}{\lambda_0} \right] + \frac{1}{2} \left(\frac{\lambda_0}{R} \right)^2 \left(\exp\left[-2\frac{R}{\lambda_0} \right] - 1 \right) \right\}. \tag{21}$$

In the limit $\sigma_{VN} \to \infty$, i. e. $\lambda_0/R \to 0$ this just reduces to

$$T_A \longrightarrow \frac{\pi R^2}{A \sigma_{VN}} . \tag{22}$$

4.2 Fit results

We now fit these expressions, using the inelastic vector meson nucleon cross section σ_{VN} as an open parameter, to our BUU calculations shown in Fig. 8 with $K_{\mathrm{inel}} = K_{\mathrm{el}} = 1$. To this end we include only nuclei starting from ^{40}Ca

since our starting point, i. e. the Glauber expression for the nuclear photo-production cross section Eq. (17), is valid only for large nuclei with a relative error of the order of A^{-1} [36,37]. The results of this procedure are shown in Fig. 11. Adopting the lowest order expression (22) we find an inelastic ωN cross section of 23 mb, whereas including the correction factor in the curled brackets in Eq. (21) an inelastic cross section of 20 mb is found. Hence, the correction terms are only of minor importance. This is particularly true for large nuclei as the additional terms come with powers of (λ_0/R) which is a small parameter for heavy nuclei and large absorption cross sections.

As said earlier, the momentum distribution of the ω mesons in the data sample is peaked around $p_V = 1$ GeV. Hence, the inelastic ωN cross section in our transport calculations with $K = 1$ amounts to roughly 24 mb, see Eq. (2). This is in astonishing agreement with the much simpler Glauber result. The somewhat smaller values extracted by means of the analytic formula (21) can be attributed to the disregard of any target surface region where the mean free path of the vector mesons again becomes large, giving rise to a diminishing absorption probability for any produced particle on its way out of the nucleus. We conclude that the Glauber model provides a quite reliable tool to extract the ωN inelastic cross section. Actual experiments, however, often have geometrical and kinematical acceptance limitations which then require the full transport calculation as we have shown for the case of ϕ photoproduction in [19].

5 Summary

In summary, we have shown that a measurement of the nuclear transparency ratio can indeed yield important information on the real and imaginary part of the ω nucleus potential. To this end we have included all nuclear effects in a coupled-channel transport calculation that describes the incoherent contribution to photon-nucleus reactions. The imaginary part of the ω in-medium self energy can be extracted from the A-dependence of the nuclear transparency ratio by fitting the total inelastic ωN cross section to experimental data. For such a measurement we consider a photon beam energy of around 1.5 GeV as optimal. Studying total inclusive observables only, the inelastic vector meson nucleon cross section can also be extracted from the naive Glauber multiple scattering result with a relative error on the $10 - 20\%$ level.

Also the real part of the ω in-medium self energy can at least in principle be studied from an examination of the energy dependence of the transparency ratio in the threshold region. Uncertainties arise from the fact that not only the intrinsic properties of the ω meson but also the ω production cross section or its decay width can experience modifications from the interaction of the

involved particles with the surrounding nuclear matter. Any statement about the real part of the ω nucleus potential has to relie on assumptions for the elementary ω production cross section. It is also important to realize that the attenuation measurement as considered in the analysis at hand is sensitive not to the ω self energy at rest but to the ω properties at rather high momenta, i. e. the momentum range around 1 GeV.

References

[1]   G. Agakichiev *et al.* [CERES Collaboration], Eur. Phys. J. C **41** (2005) 475.

[2]   G. Usai *et al.* [NA60 Collaboration], Eur. Phys. J. C **43** (2005) 415.

[3]   J. Adams *et al.* [STAR Collaboration], Phys. Rev. Lett. **92** (2004) 092301.

[4]   D. Trnka *et al.* [CBELSA/TAPS Collaboration], Phys. Rev. Lett. **94** (2005) 192303 .

[5]   K. Ozawa *et al.* [E325 Collaboration], Phys. Rev. Lett. **86** (2001) 5019.

[6]   G. E. Brown and M. Rho, Phys. Rev. Lett. **66** (1991) 2720.

[7]   T. Hatsuda and S. H. Lee, Phys. Rev. C **46** (1992) 34.

[8]   S. Leupold, W. Peters and U. Mosel, Nucl. Phys. A **628** (1998) 311.

[9]   V. Bernard and U. G. Meissner, Nucl. Phys. A **489** (1988) 647.

[10]   F. Klingl, N. Kaiser and W. Weise, Nucl. Phys. A **624** (1997) 527.

[11]   F. Klingl, T. Waas and W. Weise, Nucl. Phys. A **650** (1999) 299.

[12]   M. Post and U. Mosel, Nucl. Phys. A **688** (2001) 808.

[13]   M. F. M. Lutz, G. Wolf and B. Friman, Nucl. Phys. A **706** (2002) 431.

[14]   F. Klingl, N. Kaiser and W. Weise, Z. Phys. A **356** (1996) 193.

[15]   P. Muhlich, T. Falter and U. Mosel, Eur. Phys. J. A **20** (2004) 499.

[16]   C. Djalali *et al.* [CLAS collaboration], private communication (2004).

[17]   H. Alvensleben *et al.*, Phys. Rev. Lett. **24** (1970) 786.

[18]   D. Cabrera, L. Roca, E. Oset, H. Toki and M. J. Vicente Vacas, Nucl. Phys. A **733** (2004) 130.

[19]   P. Muehlich and U. Mosel, Nucl. Phys. A **765** (2005) 188.

[20] T. Ishikawa *et al.*, Phys. Lett. B **608** (2005) 215.

[21] M. Effenberger, E. L. Bratkovskaya and U. Mosel, Phys. Rev. C **60** (1999) 044614.

[22] P. Muhlich, T. Falter, C. Greiner, J. Lehr, M. Post and U. Mosel, Phys. Rev. C **67** (2003) 024605.

[23] B. Andersson, G. Gustafson and H. Pi, Z. Phys. C **57** (1993) 485.

[24] S. Teis, W. Cassing, M. Effenberger, A. Hombach, U. Mosel and G. Wolf, Z. Phys. A **356** (1997) 421.

[25] J. Lehr, M. Effenberger and U. Mosel, Nucl. Phys. A **671** (2000) 503.

[26] T. Falter and U. Mosel, Phys. Rev. C **66** (2002) 024608.

[27] G. Penner and U. Mosel, Phys. Rev. C **66** (2002) 055212.

[28] J. Barth *et al.* [SAPHIR collaboration], Eur. Phys. J. A **18** (2003) 117.

[29] G. I. Lykasov, W. Cassing, A. Sibirtsev and M. V. Rzyanin, Eur. Phys. J. A **6** (1999) 71.

[30] V. Shklyar, H. Lenske, U. Mosel and G. Penner, Phys. Rev. C **71** (2005) 055206 [Erratum-ibid. C **72** (2005) 019903].

[31] J. G. Messchendorp, A. Sibirtsev, W. Cassing, V. Metag and S. Schadmand, Eur. Phys. J. A **11** (2001) 95.

[32] W. Peters, M. Post, H. Lenske, S. Leupold and U. Mosel, Nucl. Phys. A **632** (1998) 109.

[33] M. Post, S. Leupold and U. Mosel, Nucl. Phys. A **689** (2001) 753.

[34] M. Post, S. Leupold and U. Mosel, Nucl. Phys. A **741** (2004) 81.

[35] S. Eidelman *et al.* [Particle Data Group], Phys. Lett. B **592** (2004) 1.

[36] R. J. Glauber *"High energy collision theory"*, in *"Lectures in Theoretical Physics Vol. 1"*, Wiley Intersience, New York (1959) 315.

[37] R. J. Glauber *"Theory of high energy hadron-nucleus collisions"*, in *"High energy physics and nuclear structure"*, Plenum, New York (1970) 207.